CrossMark

ORIGINAL PAPER

Climate change effects on wildland fire risk in the Northeastern and Great Lakes states predicted by a downscaled multi-model ensemble

Gaige Hunter Kerr[1,2] (ID) · Arthur T. DeGaetano[2] ·
Cathelijne R. Stoof[2,3] · Daniel Ward[4]

Abstract This study is among the first to investigate wildland fire risk in the Northeastern and the Great Lakes states under a changing climate. We use a multi-model ensemble (MME) of regional climate models from the Coordinated Regional Downscaling Experiment (CORDEX) together with the Canadian Forest Fire Weather Index System (CFFWIS) to understand changes in wildland fire risk through differences between historical simulations and future projections. Our results are relatively homogeneous across the focus region and indicate modest increases in the magnitude of fire weather indices (FWIs) during northern hemisphere summer. The most pronounced changes occur in the date of the initialization of CFFWIS and peak of the wildland fire season, which in the future are trending earlier in the year, and in the significant increases in the length of high-risk episodes, defined by the number of consecutive days with FWIs above the current 95th percentile. Further analyses show that these changes are most closely linked to expected changes in the focus region's temperature and precipitation. These findings relate to the

current understanding of particulate matter vis-à-vis wildfires and have implications for human health and local and regional changes in radiative forcings. When considering current fire management strategies which could be challenged by increasing wildland fire risk, fire management agencies could adapt new strategies to improve awareness, prevention, and resilience to mitigate potential impacts to critical infrastructure and population.

1 Introduction

Regional meteorology drives the conditions conducive to increased wildland fire risk through mechanisms such as high temperatures, elevated surface winds, nominal precipitation, and decreased soil moisture and is also responsible for the non-anthropogenic source of wildland fire ignition, lightning (Flannigan et al. 2005). While wind is a mechanism by which wildland fires experience growth, Parisien et al. (2011) examined several environmental factors related to wildland fires in North America and suggested that extreme temperatures most strongly governed wildland fire activity. Regional fire regimes are highly sensitive to climate change due to an immediate response on fuel moisture from changes in precipitation, temperature, wind speed, and relative humidity (Moriondo et al. 2006). Pronounced climatic changes have already begun to alter the long-standing climatic averages of the Northeastern and Great Lakes states in the USA (henceforth "focus region") and these changes are expected to continue through the twenty-first century (e.g., Hayhoe et al. 2007; Gao et al. 2012; Ning et al. 2015). Knowledge of the impact of these climatic changes on fire regimes in this historically non-fire-prone region is essential for sound preparation for these changes by land managers, fire professionals, and policy makers.

✉ Gaige Hunter Kerr
  gaige.kerr@jhu.edu

[1] Department of Earth & Planetary Sciences, The Johns Hopkins University, Baltimore, MD 21218, USA

[2] Department of Earth and Atmospheric Sciences, Cornell University, Ithaca, NY 14853, USA

[3] Soil Geography and Landscape Group, Wageningen University, PO box 47, 6700 AA Wageningen, The Netherlands

[4] Department of Atmospheric and Oceanic Sciences, Princeton University, Princeton, NJ 08544, USA

The key objectives of this study are to spatially, temporally, and statistically quantify expected changes in wildland fire risk and thereafter consider the most important climatic factors driving these changes. We use regional climate models (RCMs) dynamically downscaled by a subset of general circulation models (GCMs) from Phase 5 of the Coupled Model Intercomparison Project (CMIP5) (Taylor et al. 2012) as inputs to the Canadian Forest Fire Weather Index System (CFFWIS) (Wagner 1987). The public perceptions of currently low wildland fire risk (Hawbaker et al. 2013) and heavy urbanization (2013) in this focus region make it an important region to study the effects of climate change on wildland fire risk to provide an accurate overview for impact assessment and policy development. We begin this paper with an overview of the synoptic meteorological patterns affecting the focus region as well as a brief description of the general climatic conditions (Section 2.1). This is followed with a description and framework for the regional climate and fire weather models used in this study (Sections 2.2 and 2.3). Section 2.4 expands on the metrics applied to understand changes in wildland fire risk. Section 3 focuses on the significant effects of climate change on wildland fire risk, and we discuss the extent to which uncertainties may confound these effects. Finally, we summarize our findings (Section 4) and call for a better understanding of additional factors that contribute to wildland fire risk and effective adaptation techniques.

2 Data and methods

2.1 Focus region

We define our focus region based loosely on the amalgamation of two ecoregions defined by the Joint Fire Science Program (JFSP) (see www.firescience.gov). Here, we consider the Great Lakes states to be Minnesota, Wisconsin, Michigan, and Ohio. The Northeastern states include Pennsylvania, New York, Vermont, New Hampshire, Maine, Massachusetts, Connecticut, Rhode Island, New Jersey, Delaware, and Maryland (Fig. 1). The climate of the region is diverse due, in part, to several geographic factors. The Atlantic Ocean and Great Lakes regulate the climate of nearby areas as well as influence mesoscale weather patterns. The sheer size of the Great Lakes reduces the diurnal and annual variation of air temperature and also alters cloud cover and downwind precipitation patterns (d'Orgeville et al. 2014). Average annual precipitation substantially varies across the focus region ranging from about 600 mm yr^{-1} in Minnesota to 1300 mm yr^{-1} in New England coastal areas. The Appalachian Mountains, a narrow system of mountains running parallel to the eastern seaboard and generally considered to be the geographical line which divides the eastern

seaboard of the USA with the Midwestern region, are orographic influences and increase precipitation. Some highly localized areas in these mountainous regions annually receive over 1500 mm of precipitation (Kunkel et al. 2013a, b).

Climatological records in the Northeastern states reveal frequent heat waves (defined as three or more days of temperatures exceeding 32 °C) occurring nearly annually during the summer (Kunkel et al. 2013b). Northeastern meteorological droughts occur less frequently, on average every 2–3 years, and have a temporal scale of 1–3 months (Kunkel et al. 2013b). Changing temperature patterns are expected to cause milder winters and more extreme heat events during the summer (Thibeault and Seth 2014). Multi-model averages from 23 coupled models project warm spells in the Northeast to lengthen more than 700 % by the middle of the twenty-first century and more than 1500 % by the late twenty-first century over 1951–2010 values (Thibeault and Seth 2014). An analysis of precipitation across the Northeastern states since 1970 has shown upward trends in annual amounts and greater variability (Kunkel et al. 2013b). The seasonal distribution of future precipitation in the Northeast is expected to shift to higher amounts during the winter season with decreases or no changes during the summer season (Hayhoe et al. 2007).

In the Great Lakes states, the distribution of precipitation is also changing. By mid-century, a median increase of between 14 and 29 % in the frequency of a 50-year rainfall event is expected to occur (d'Orgeville et al. 2014). However, these states will still experience, overall, drier conditions (Swain and Hayhoe 2015) as precipitation will fall during temporally brief, extreme precipitation events. Similar to the Northeastern states, the Great Lakes states can anticipate average daily maximum temperatures to increase by 3–6 °C by the end of the century (Wuebbles and Hayhoe 2004). Summertime temperature changes at the end of the century under a high emission scenario are anticipated to be the highest in Minnesota and Wisconsin (Wuebbles and Hayhoe 2004). The highest upward trends in precipitation are projected in Minnesota while no change is expected in the Eastern Great Lakes states such as Michigan and Ohio (Wuebbles and Hayhoe 2004). Modeled summer temperatures and precipitation distributions in Upper Great Lakes states are expected to resemble current summer conditions in Arkansas or Mississippi (Wuebbles and Hayhoe 2004).

Along with expected temperature and precipitation changes, the duration of the frost-free season is changing across the entire focus region. For boreal and temperate forests, studies have reported similar trends in spring onset and leaf-out, which are shifting earlier in the year (Schwartz et al. 2006; Schwartz et al. 2013; Ault et al. 2015). Although the responses of leaf senescence and leaf abscission to climate change have not been thoroughly researched and autumn has been referred to as the "neglected season in climate change

research" (Gallinat et al. 2015), several studies investigated the frost-free season as a whole and found statistically significant trends in the increasing length of the frost-free season (Wuebbles and Hayhoe 2004; Kunkel 2004; Kunkel et al. 2013b). In subsequent sections of this manuscript, we consider this changing length of the frost-free season to explain our findings in future projections of FWIs in the focus region.

2.2 The Canadian Forest Fire Weather Index System

The Canadian Forest Fire Weather Index System (henceforth "CFFWIS"), developed by the Canadian Forestry Service, has been in use since 1970. Changes in units and various mathematical procedures occurred in the years following 1970, but the overall continuity of the output has been preserved (Wagner 1987). CFFWIS synthesizes meteorological parameters to estimate the effects of weather on wildland fire risk but does not take into account other factors contributing to risk (e.g., biomass, ignitions, topography, etc.) (DeGroot et al. 1998). CFFWIS was calibrated and tested in Canadian boreal forests and represents a standardized fuel type characterized by mature Jack Pines (*Pinus banksiana*) and Lodgepole Pines (*Pinus contorta*) (Wotton 2009; Chelli et al. 2015). Although CFFWIS historically was used as an operational model, it has been widely used for climate-related research applications in many different fire regimes beyond Canada's boreal forests such as the Daxing'anling region of China, the Mediterranean Basin, and Australia (Tian et al. 2011; Moriondo et al. 2006; Clarke et al. 2013).

CFFWIS uses daily measurements of air temperature, relative humidity, instantaneous wind speed, and accumulated precipitation taken at 1200 h local standard time (LST) to determine six indices which represent fuel moisture, the rate of fire spread, and fuel weight consumed (Wagner 1987). 1200 h LST observations input to the model predict wildland fire conditions during the peak time of fire activity, around 1600 h LST, if daily air temperature, relative humidity, and wind speed follow typical diurnal patterns (Turner and Lawson 1978; Wagner 1987). Within CFFWIS, latitude is used to determine daylength. Outputs of CFFWIS include three moisture indices (fine fuel moisture code, duff moisture code, drought code), two indices pertaining to fuel moisture influences on wildland fire behavior (initial spread index, buildup index), and an index which represents the intensity of a spreading fire (fire weather index) (Turner and Lawson 1978). The fire weather index (FWI) is considered to be a "first level" index and combines the effects of the other indices into one numerical value (Wagner 1987) which is a measure of the rate of a fire's spread with the amount of fuel consumed. This index is suitable for a general measure of wildland fire risk (Lawson and Armitage

2008). Within our research, it is the component of CFFWIS that we compute and analyze.

Persistent meteorological conditions are factored into the daily calculations of the FWI: CFFWIS uses the previous day's moisture indices to calculate the FWI. The seasonal starting procedure for CFFWIS varies and is contingent upon either snow cover or daily temperature values (Turner and Lawson 1978). Since correct simulations of snow cover have been only partially reproduced by state-of-the-art climate models (Brutel-Vuilmet et al. 2013), our starting procedure was based on Natural Resources Canada's recommendation of initializing CFFWIS when the daily mean temperature is at least 6 °C for three consecutive days. When this criterion was met, CFFWIS was initialized and start-up values were calculated for the moisture indices based on the number of days since the last precipitation fell. This initialization should not be confused with the onset of northern hemisphere spring. Although it could indicate warmer winter temperatures, it could also indicate a brief warm spell. Daily mean temperature is not a variable included within the framework of the Coordinated Regional Climate Downscaling Experiment (CORDEX), so the approach of Forsythe et al. (1995) was used to calculate daylength, and subsequently, a diurnal temperature curve from daily maximum near-surface air temperature ($tasmax$) and daily minimum near-surface air temperature ($tasmin$) was constructed and averaged to yield the daily mean temperature. In the event that start-up values are over- or underestimated, the fine fuel moisture code will correct itself after about 3 days (Turner and Lawson 1978). In this research, we calculated and analyzed daily FWIs from the date of initialization of CFFWIS until the end of the calendar year due to the aforementioned increases in the length of the frost-free season that prevented the use of a temperature threshold. A standard method of calculating the official end of the fire season does not exist (Wotton and Flannigan 1993). Some have calculated the end of the season based on temperature thresholds, while others stop daily calculation when contracts end for seasonal employees working for fire management agencies (Wotton and Flannigan 1993).

2.3 Regional climate scenarios

We assessed twentieth century simulations and twenty-first century projections of wildland fire risk using the latest set of coordinated climate model intercomparison experiments, CMIP5 (Taylor et al. 2012). In particular, we relied on CORDEX to provide reanalyses, historical simulations, and future projections of dynamically downscaled regional climate scenarios for North America (Giorgi et al. 2009). There are a variety of regional simulations available for the CORDEX North American domain from several modeling groups, and we selected a subset of these simulations based

on their temporal frequency, high grid cell resolution (0.44°, ≈ 50 km), and high greenhouse gas concentrations. Since wildland fire risk has a high temporal variability, we deemed it necessary to only evaluate regional simulations available at a daily frequency. Previous wildland fire risk studies have exclusively used high-emissions scenarios (e.g., Goff et al. 2009; Clarke et al. 2011), and current trends in global emissions show yearly increases which align with these "business as usual" scenarios (Peters et al. 2013). Our greenhouse gas concentration criterion is therefore based upon the Representative Concentration Pathways (RCP) raising radiative forcing by 8.5 W m^{-2} due to anthropogenic emissions by 2100 (Moss et al. 2010; van Vuuren et al. 2011). These criteria resulted in our use of the models shown in Table 1 combined in a multi-model ensemble (MME) with a "one model, one vote" approach. We chose this approach because examining individual ensemble members, on their own, may lead to error due to differing parameterizations, boundary conditions, and initial conditions; however, using a MME improves the reliability, skill, and consistency of predictions (Tebaldi and Knutti 2007) and provides a measure of likelihood of projected risk (Kendon et al. 2008). Unless noted, all subsequent plots and figures show the results of the MME rather than the individual CORDEX models.

CORDEX provides reference data for evaluation, the ERA-Interim driven reanalysis (Dee et al. 2011). RCMs driven by reanalyses are available for 1989–2012, and RCMs driven by historical simulations are available for 1951–2004. We examined the overlapping period between the reanalyses and the historical simulations (1989–2004) to assess model performance and to ensure that the RCMs driven by GCMs accurately portray the reanalyses without producing artificial trends or other artifacts. We defined

Table 1 Regional simulations from the CORDEX North American domain (Giorgi et al. 2009) used in this study

RCM	Driving reanalysis ERA-Int	Driving GCM CanESM2	EC-EARTH
RCA4	X	X	X
CanRCM4	X	X	
HIRHAM5	X		X

The regional climate models (RCMs) include (1) Sveriges Meteorologiska och Hydrologiska institut (SMHI) Rossby Centre Regional Atmospheric Climate Model, version 4 (RCA4), (2) Centre canadien de la modélisation et l'analyse climatique/Canadian Centre for Climate Modelling and Analysis (CCCma) Canadian regional climate model, version 4 (CanRCM4), and (3) Danmarks Meteorologiske Institut HIRHAM, version 5 (HIRHAM5). The general circulation models (GCMs) and reanalyses include (1) European Centre for Medium-range Weather Forecast (ECMWF) Interim Reanalysis (ERA-Int), (2) second generation Canadian earth system model (CanESM2), and (3) ECMWF/Europe-wide consortium earth system model (EC-EARTH)

this period as a baseline for several metrics related to wildland risk. The CORDEX future scenario spans 2006–2100, and in addition to trends aggregated over this entire period, two arbitrary 25-year periods, a mid-century period (2026–2050), and a late-century period were examined. For additional details about the CORDEX experimental design, refer to http://www.cordex.org.

From CORDEX, we obtained $tasmax$, $tasmin$, 12 UTC near-surface specific humidity (q), 12 UTC surface pressure (ps), near-surface wind speed ($sfcWind$), and 12 UTC accumulated precipitation (pr). Daily values of relative humidity were computed by combining $tasmax$, q, and ps in the classical Clausius-Clapeyron relationship (Lawrence 2005).

We began our investigation with a systematic comparison of FWIs produced with the ERA-driven reanalysis from CORDEX and FWIs produced with local observations. Research has revealed biases and lack of model consensus in CMIP5 GCMs which effectively decrease confidence in future climate projections (Maloney et al. 2014). We sought to investigate whether these biases—or biases present in the RCMs—would yield different FWIs compared to those produced with meteorological observations. Figure 1 compares daily FWIs produced with hourly meteorological observations from CLIMOD (climod.nrcc.cornell.edu) for the measuring period 1989–2004 versus the MME from the ERA-driven reanalysis calculated in the same manner as elsewhere in this paper. Sites examined represent stations across the Northeastern and Great Lakes states with reliable, complete climatic records and are identifiable in Fig. 1a with black scatter points and in Fig. 1b–k by their ICAO codes. In an effort to smooth out any noise in the ERA-driven reanalysis, the reanalysis was sampled at the five nearest grid cells to the stations' locations and averaged; these grid cells are shown in blue in Fig. 1a. Upon comparing the signal and noise in the box plots in Fig. 1b–f, we note similar first quartiles, median, and minimum values for selected sites. Indeed, by definition the FWI has a minimum of 0 corresponding to very low risk, so these whiskers correspond to 0 or near-zero values. The variability and maximum values of FWIs produced with observations versus the reanalysis are slightly greater in magnitude. The cumulative distribution functions (CDFs), shown in Fig. 1g–k, compliment the findings in the box plots and give validity to the notion that FWIs produced in these two different manners have similar distributions, although FWIs derived from the reanalysis leads to a slight underestimation of FWIs for CDF values between 0.4 and 1. Overall, this systematic comparison at these sites revealed that FWIs produced with the ERA-driven reanalysis from CORDEX slightly underestimated wildland fire risk. Additional analyses (not shown) indicated that the seasonal cycle of FWIs computed through observations versus CORDEX was largely preserved. For
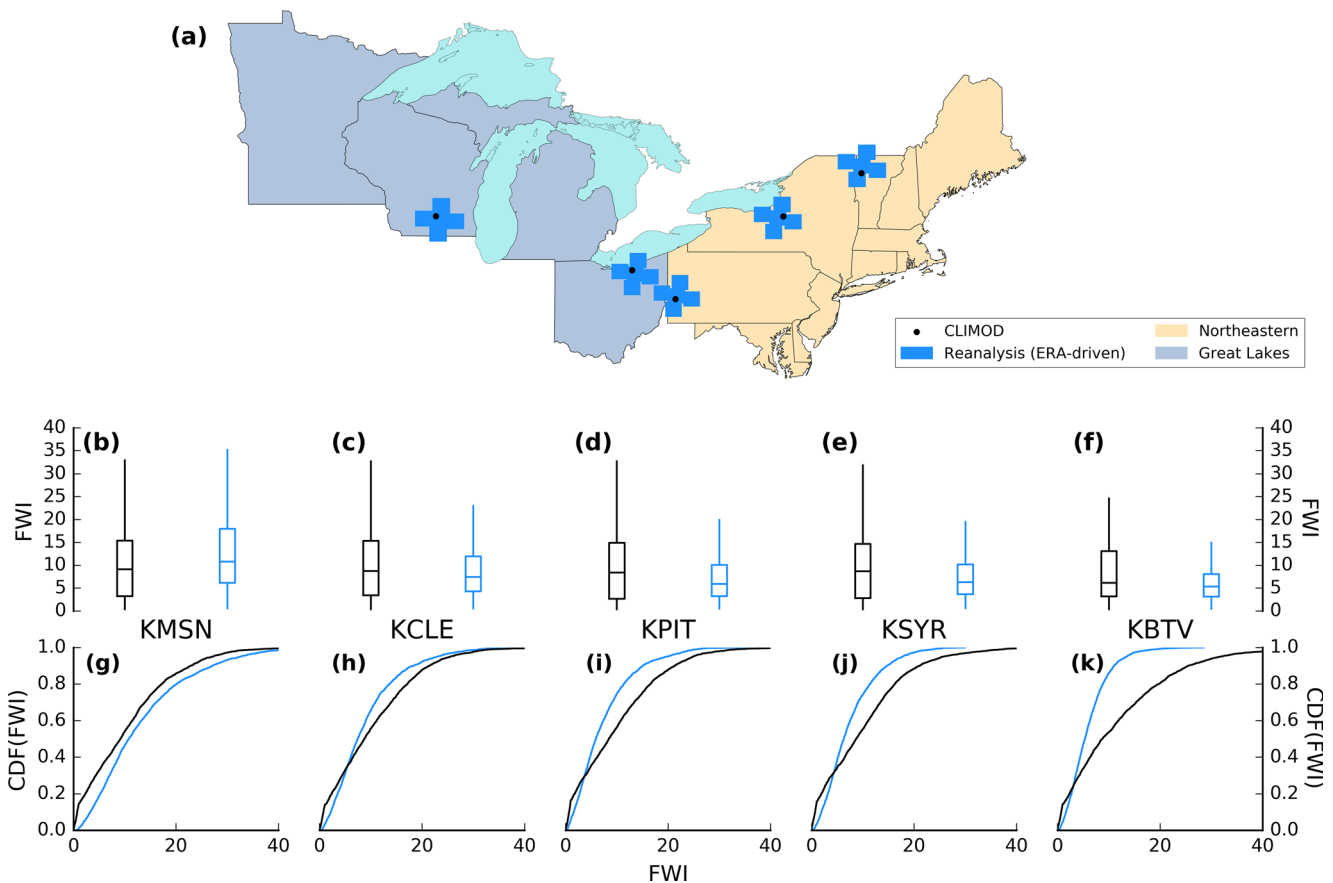
Fig. 1 Comparison of observed and modeled Fire Weather Indices (FWIs). The locations of observed FWIs shown in a, derived from hourly, derived from hourly meteorological observations at select sites, are shown as scatter points while ERA-Interim grid cells which, averaged, yielded the FWIs derived from the reanalysis are shown as patches. Also shown in **a** are the Northeastern and Great Lakes states referred to extensively in this paper. Boxplots of FWIs computed with observations and the reanalysis over the historical period (1989–2004) are shown in **b–f**. Indicated on the boxplots (from *bottom*) are the minimum value, 1st quartile, median, 3rd quartile, and the maximum value. Subplots (**g–k**) show cumulative distribution functions (CDFs) of observed and modeled FWIs for the same stations and measuring period

these reasons, we did not deem it necessary to apply any offset or scale factor to our results from CORDEX.

2.4 Data analysis

In this study, we use several metrics to gauge projected changes in wildland fire risk. The metrics chosen for analysis are as follows: (1) *Magnitude of FWIs.* Daily FWI values averaged over the historical, mid-century, and late-century periods show the annual cycle of the wildland fire season and expected changes in the magnitude of FWIs corresponding to increased wildland fire risk. (2) *Temporality of the fire season.* Given the recent trends in spring onset (e.g., Schwartz et al. 2006, 2013; Ault et al. 2015), what are their effects on the timing of the fire season? We investigated trends in the date of the start and peak of the wildfire season, defined as the date of initialization of CFFWIS and maximum FWI in a year, respectively. (3) *Changing length of high-risk episodes.* We examined the right tail of the FWI distribution and, in particular, the 95th percentile of FWIs

as this portion of the distribution corresponds to days where more frequent, extreme fires could occur (Wang et al. 2015). We define a "high-risk day" in our focus region as a day which exceeds the 95th percentile for historical FWIs. We then examine the largest consecutive number of days in a year where this threshold is exceeded.

Statistical comparison of spatial fields FWIs computed from ERA-Interim driven reanalysis were compared to FWIs computed from CORDEX historical simulations by a test for differences of mean for paired samples for auto-correlated data (Wilks 2011). Statistical significance was assessed by z-scores at the 95 % confidence level under a null hypothesis of zero change; here, z is defined by:

$$z = \frac{\overline{\Delta} - \mu_\Delta}{(s_\Delta^2 / n')^{1/2}} \tag{1}$$

where $\overline{\Delta}$ is mean of the $\overline{FWI}_{CORDEX}$ and $\overline{FWI}_{ERA-Interim}$ paired differences, $\mu_\Delta = 0$ under the

null hypothesis, and s_Δ^2 is the sample variance of the paired differences. Since using the previous day's FWI to calculate the present day's FWI introduces time dependence, an effective sample size (n') was determined using the approximation:

$$n' \approx n\frac{1-\rho_1}{1+\rho_1} \qquad (2)$$

where ρ_1 is the lag-1 autocorrelation coefficient.

Trend detection in the seasonality of wildland fire risk
Typically, Spearman's rho test or the non-parametric Mann-Kendall trend test is used to analyze possible temporal trends in data (Wilks 2011). For this study, the Mann-Kendall trend test was invoked to assess the significance in the nonstationarity of the time series and the degree of association between time and parameter of interest. The high interannual variability of the metrics related to wildland fire risk results in a non-normal distribution for which the Mann-Kendall is particularly appropriate. The null hypothesis for the Mann-Kendall trend test is that the data have no trend or serial correlation (Hamed and Rao 1998). The test statistic is discussed in detail by Wilks (2011) and given as:

$$S = \sum_{i=1}^{n-1}\sum_{j=i+1}^{n} sgn(x_j - x_i) = \sum_{i<j} sgn(x_j - x_i) \qquad (3)$$

where:

$$sgn(\Delta x) = \begin{cases} +1, & \Delta x > 0 \\ 0, & \Delta x = 0. \\ -1, & \Delta x < 0 \end{cases} \qquad (4)$$

If some values in the data are repeated, the variance of the distribution varies directly with these non-distinct values; the variance is defined by:

$$Var(S) = \frac{n(n-1)(2n+5) - \sum\limits_{j=1}^{J} t_j(t_j-1)(2n+5)}{18} \qquad (5)$$

Finally, the z test statistic, a standard Gaussian value, is computed and used to evaluate the test p value.

$$z = \begin{cases} \frac{S-1}{[Var(S)]^{\frac{1}{2}}}, & S > 0 \\ \frac{S+1}{[Var(S)]^{\frac{1}{2}}}, & S < 0 \end{cases} \qquad (6)$$

3 Results and discussion

Since the FWI is a strong indicator of wildland fire risk in forested areas (Lawson and Armitage 2008), our results show that future climate changes will more frequently trigger conditions conducive to wildland fires through enhanced FWIs. The upper left subplot in Fig. 2 shows linear trends

in the magnitude of the annual maximum FWIs from 1989–2100. In this subplot, the largest trends in the magnitude of FWIs are concentrated in a broad swath along the northern border of the focus region (i.e., Michigan's Upper Peninsula, northern Minnesota, New York). Negative trends, smaller in absolute value than the projected positive trends, are noted in the far western portions of the focus region (southern Minnesota). The remaining three subplots in Fig. 2 depict mean annual maximum FWIs for the three periods of interest. The geographic distribution of larger versus smaller FWIs does not change in a major way between the historical and late-century periods, rather we observe nuanced increases in the magnitude of FWIs. The large magnitudinal range of FWIs that exists in the focus region make detecting differences between the three time periods in the remaining subplots of Fig. 2 difficult. However, projected changes in the magnitude of annual maximum FWIs, in some cases, represent 100 % increases.

Stippling in the upper right subplot of Fig. 2 corresponds to statistically significant differences between annual maximum FWIs produced with CORDEX historical simulations and the ERA-Interim driven reanalysis at the 95 % confidence level and was determined with t tests for autocorrelated data (Eqs. 1 and 2). These differences manifest themselves as biases between historical CORDEX simulations and the ERA-Interim driven reanalysis in Fig. 3. For both the Great Lakes and the Northeastern states in springtime, FWIs produced with historical CORDEX simulations and ERA-Interim driven reanalyses are roughly the same. However, during the latter half of the year, FWIs are slightly overestimated by CORDEX historical simulations. In the Northeast, this overestimate is apparent starting in mid-June and lingering until October. Whereas for the Great Lakes states it is limited to, more or less, a 3 month window: July through September. These differences do not have to underscore our method of investigating changes in wildland fire risk: although forcing RCMs with GCMs can lead to errors due to incorrect boundary conditions and structural biases, studies over the CORDEX North American domain have shown skill in reproducing near-surfaces fields as well as in simulating mesoscale and synoptic climatic features (Martynov et al. 2013; Šeparović et al. 2013). In the CORDEX models investigated by Martynov et al. (2013), there is good agreement between historic simulations and observation-based datasets, and they assert that the performance of CORDEX in simulating historic near-surface atmospheric processes is a sound basis for projecting future climate. In our study, we thus assume that the biases present in CORDEX historical simulations persist in CORDEX future projections; therefore, presenting the changes between the future projections relative to the historical simulations allows accurate assessment despite the biases as the focus is on relative changes.

Fig. 2 Linear trends and changes in FWIs. Linear trends in the annual maximum FWIs are shown *(upper left)*. The remaining subplots show annual maximum FWIs averaged over the baseline, mid-century, and late-century periods. Stippling in the baseline subplot *(upper right)* corresponds to statistically significant differences between ERA-Interim and CORDEX historical simulations at the 95 % confidence level
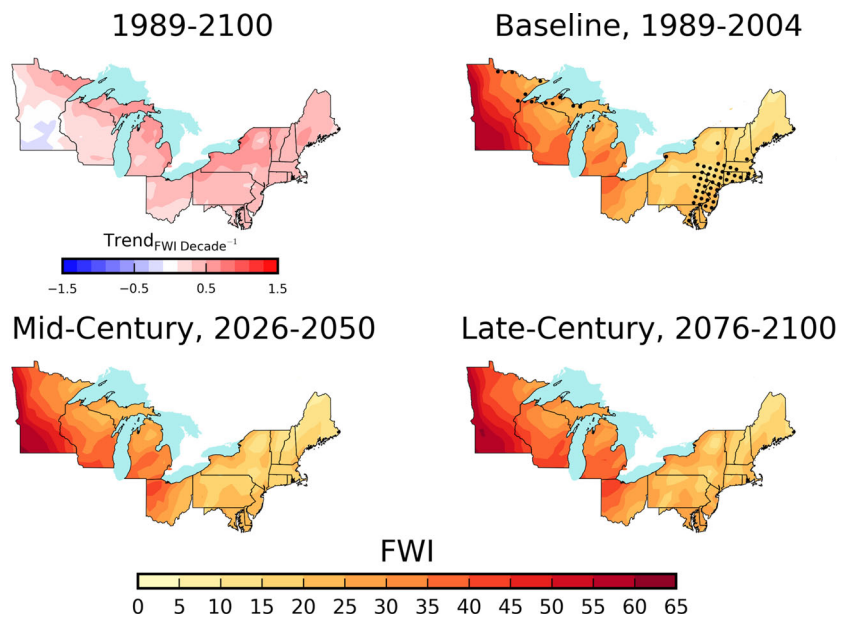
Possible biases arising from time dependence and the memory in CFFWIS necessitated a resampling test to construct batches of artificially paired data to determine how unlikely the number of statistically significant different grid cells we observed was. FWIs were therefore resampled in a way that was consistent with the null hypothesis that no statistical difference existed between FWIs computed with CORDEX historical simulations versus those driven by the ERA-Interim reanalysis. We constructed a collection (1000 realizations) of artificial data and found test statistics with the aforementioned t tests for autocorrelated data. From here, we compared these with the statistics from the original data to investigate the significance of our original findings. Upon comparing the total number of grid nodes where

statistically significant differences existed for our original data and the artificial data, we see that our original findings lie in the critical region ($\alpha = 0.99$) of the left tail of the distribution; thus, the resampling test gives strong evidence that our findings are significant (Wilks 2011).

Figure 3 shows the seasonality of FWIs for the periods of interest. Grey lines correspond to FWIs averaged over the time periods. Colored lines were smoothed with a least squares polynomial and regularize the noisy patterns. Fire risk during the summer increases with each successive time period across the entire focus region. Differentiating changes in the magnitude of FWIs between the historical, mid-century, and late-century periods during the early and late parts of the year (January–May and

Fig. 3 The seasonal cycle of FWIs. Annual patterns for the historical, mid-century, and late-century periods are depicted in this figure along with a comparison between historical simulations and those driven by the ERA-Interim reanalysis. *Grey lines* represent daily values averaged over the respective periods while *colored lines* shown in the legend correspond to a smoothing of the grey lines with a least squares polynomial
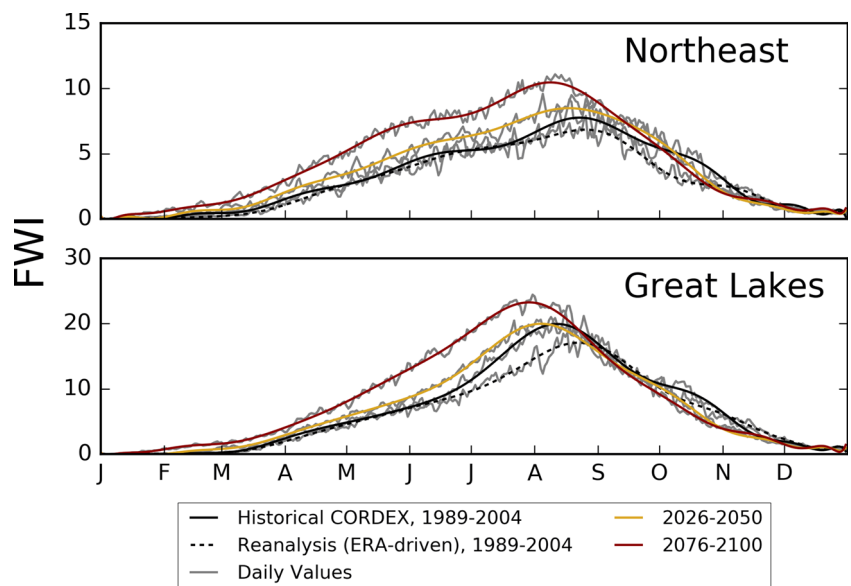
Fig. 4 Violin plot of the distribution of FWIs. These violin plots combine box plots with kernel density estimations to show the changing distribution of FWIs in the twenty-first century for the Northeastern and Great Lakes states. The *upper row* corresponds to the multi-model ensemble average calculated with the "one model, one vote" approach while the *bottom four rows* give a model-by-model analysis
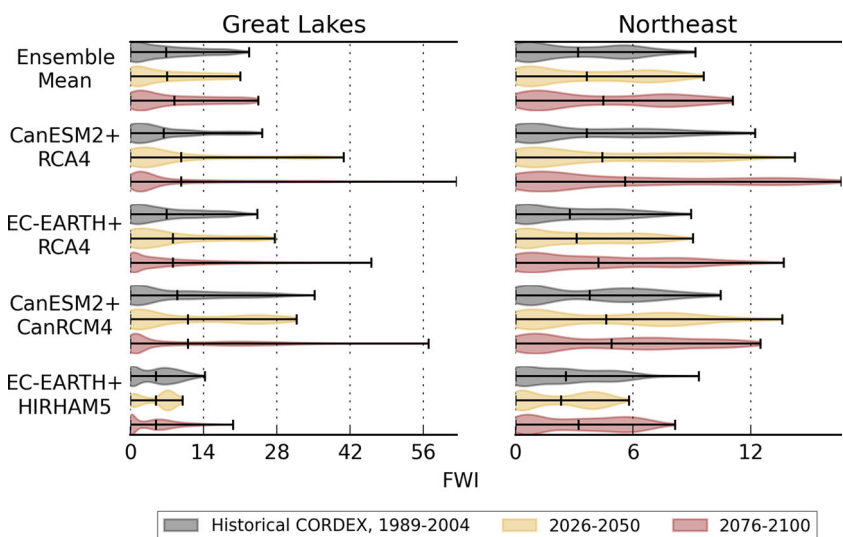
September–December) proves difficult, and often changes are not readily observable. However, pronounced changes in the magnitude of FWIs are evident during the summer. The magnitude of FWIs in the Great Lakes states, especially during the summer, is often double the magnitude found in the Northeastern states. This difference in magnitude is not only apparent in the seasonality of FWIs in Fig. 3 but also in the distribution of FWIs in Fig. 4 as FWIs in the Great Lakes states are generally more than double the value of FWIs in the Northeastern states. The violin plot (Fig. 4) illustrates obvious discrepancies when comparing individual models. Most apparent are the differences in magnitude of FWIs with EC-EARTH + HIRHAM5 (defined in Table 1), which consistently produced smaller FWIs for both the Northeastern and Great Lakes states. The performance of this model in the Northeastern states, as shown in Fig. 4, projects that the extrema, corresponding to higher risk, are projected to decrease from the historical period to mid-century period although the distribution of FWIs during the late twenty-first century in these states for this model indicates a larger number of days will have higher FWIs compared to the historical period. This model's performance is an outlier, and the other three models and the MME mean suggest that both the extrema and overall distribution of FWIs are changing in a way that is conducive to increased risk. The performance of EC-EARTH + HIRHAM5 in the focus region and, to a lesser extent, CanESM2 + CanRCM4's performance in the Northeast imply a bimodal distribution (Fig. 4). In these cases, we observe a peak of values of FWIs clustered around 0 (presumably during early spring and late fall) and a peak between the median (represented by black tick marks on the violins) and maximum. For many models in Fig. 4, the median of the distribution steadily increases for each successive period of interest. An interesting feature of the models' performance in the Great Lakes states, perhaps

explained by interdecadal variability, is a decrease of FWI extrema during the mid-century period with respect to the historical period and then an increase during the late-century period. This behavior is present in two of the models (i.e., CanESM2 + CanRCM4, EC-EARTH + HIRHAM5) and in the MME mean as shown in Fig. 4.

Figures 5 and 6 indicate linear trends in both the initialization of CFFWIS and the peak of the fire season. We investigated these possible trends with the Mann-Kendall trend test (Eqs. 3, 4, 5 and 6), and this test yielded evidence for significant change with time. Trends in both the Northeastern and Great Lakes states suggest that the date of initialization will occur more than 30 days earlier from the dates observed in the late 1980s. We observed similar trends in the date of the peak of the fire season across the focus region. Figure 6 shows spatial results in the trends of the date of initialization and peak of the wildland fire season. The trends of the initialization (shading in Fig. 6) appear to roughly lie in a latitudinal gradient with an earlier start of the fire season at higher latitudes. There are no areas of the focus region in which the fire season is projected to start later in the year. The spatial distribution of trends of the date of the peak (stippling in Fig. 6) are highly varied in space. For the most part, the projected behavior in the date of the peak is trending earlier in the year: only in the coastal Atlantic region do we observe this date to not change or trend later in the year. The date of initialization by the end of the century appears anomalous, coming as early as mid-January in the Northeast. Since the initialization of CFFWIS occurs when the mean daily temperature is at least 6°C for three consecutive days, our results indicate more frequent warm spells interrupting northern hemisphere winter or overall warmer winter temperatures.

The magnitude of the trends in the date of initialization are roughly the same as the magnitude of the trends

Fig. 5 Linear trends in the dates of the initialization of the Canadian Forest Fire Weather Index System (CFFWIS) and peak of the wildland fire season. These time series, in *grey*, indicate the day of the year since January 1 (DOY) of the initialization of CFFWIS and the date of maximum FWI occurrence, corresponding to the peak of the wildland fire season. The *colored lines* correspond to linear trends for the two parameters
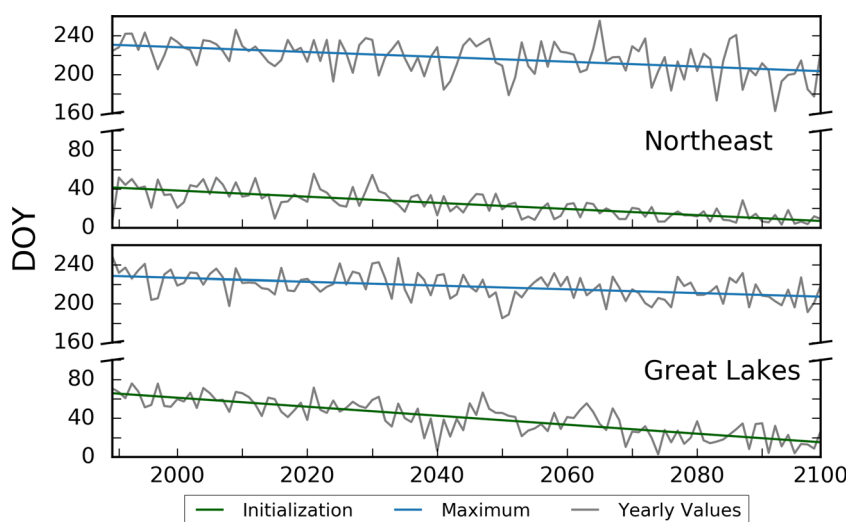
in the date of the peak (note parallel trend lines in Fig. 5), and thus the length between them is approximately the same. In Fig. 3, we observe that FWIs decrease to low values in approximately mid-November, regardless of the time period. Combining this with the earlier dates of initialization and peak could result in a longer fire season and increased risk. Similar findings were found by Flannigan et al. (2005). The expected changes in the length of the fire season could challenge the mobilization of wildfire management agencies and force them to reconsider their approach in dealing with changing fire regimes. Our findings of an earlier initialization of CFFWIS agree with a previous study by Wotton and Flannigan (1993). Of course, the exact fire risk not only depends on climate but also on fuels and ignitions. Earlier climate conditions conducive to fire affect fire occurrence will therefore be determined by the interaction between this change in climate and potential changes in fuels (type, connectivity, availability) and ignitions (frequency, location, probability).

The largest number of consecutive days above the 95th percentile for each year is shown in Fig. 7. Unlike previous studies (e.g., Guang et al. 2011) that used ordinal variables (low, moderate, high, extreme) to rank wildland fire risk, we decided to exclusively use expected changes in the annual number of consecutive days above the historical 95th percentile to correspond to high-risk periods (Fig. 7). Because of large differences in the magnitude of FWIs across the focus region, implementing a universal set of ordinal variables could lead to stark differences in what is considered low, moderate, or high risk at different locations. Thus, our use of the 95th percentile in the method of Clarke et al. (2013) and Wang et al. (2015) standardizes the classification of extreme risk throughout our domain. We additionally performed a Mann-Kendall test, and the results of this test indicate the trend (Fig. 7) for the entire focus region is significant. The analysis of this metric, shown in Fig. 7, revealed that the length of these high-risk episodes will double by 2100 over 1980s levels, thus indicating longer periods

Fig. 6 Spatial depiction of linear trends in the dates of the initialization of CFFWIS and peak of the wildland fire season. Same as Fig. 5 with shading indicating linear trends in the initialization of CFFWIS and stippling indicating linear trends in the peak of the wildland fire season
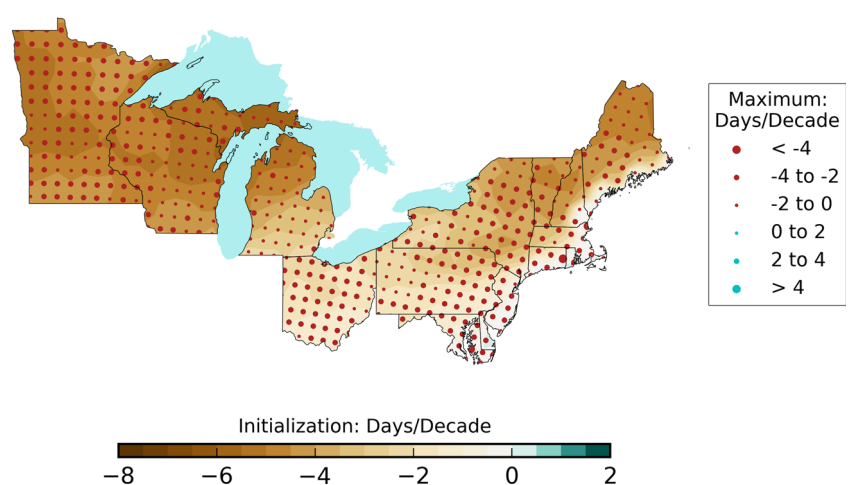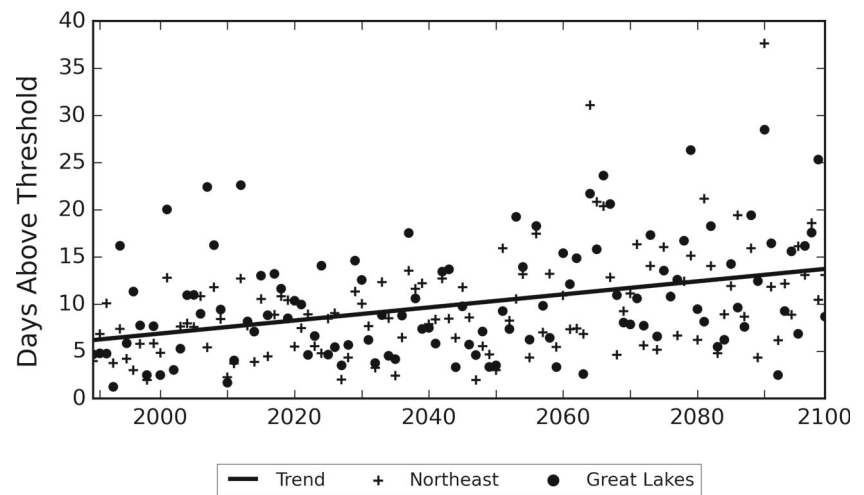
Fig. 7 Number of consecutive days exceeding the 95th percentile. *Scatter points*, averaged over the states in either the Northeast or Great Lakes regions, represent the longest period of consecutive days in a year surpassing the 95th percentile of historical FWIs. The linear trend line corresponds to expected changes aggregated across the entire focus region

conducive for wildland fire activity. Recent studies on climate extremes (Seneviratne et al. 2012) suggest that this surge in consecutive days above the 95th percentile aligns with the expected changes in the length and severity of heat events and meteorological droughts.

Furthermore, we conducted a perturbation experiment to understand the influence of biases in the input variables to CFFWIS between the historical period and future periods. Even with our approach of comparing changes between the historical and future periods, CFFWIS could react nonlinearly to biases and confound the signals seen in several of the analyses conducted. We broadly applied changes to each of the input variables from the historical period (1989–2004) and recalculated FWIs with these perturbed inputs. To do so, we scaled the input variables to the CFFWIS by simple percentage decreases (75 %) and increases (125 %) at every grid cell for the entire time period. While it is unlikely that a bias in the modeled data would present itself in this way without variance or localization, this approach gives us an estimate to first order of how the FWI reacts to changes in the input variables. Figure 8 uses a kernel density estimation to show the results of this experiment aggregated over the Northeastern and Great Lakes states. Statistical analyses (i.e., ANOVA) were performed to assess differences between the FWIs computed with perturbed inputs versus FWIs computed with the unperturbed inputs. For temperature and wind shown in Fig. 8a, c, scaling the input variables by 125 % (75 %) leads to increases (decreases) of the mean and variance of a similar magnitude as the initial perturbation, graphically shown in Fig. 8. We obtained similar results for relative humidity and precipitation in Fig. 8b, d, although perturbations to precipitation led to even smaller changes in its mean, variance, and other statistical parameters. Based on the results of this experiment, we garner an idea of the uncertainty in our projected changes through the sensitivity of the CFFWIS to systematic perturbations in the model's input variables. Further work focusing on the

sensitivity of CFFWIS is needed, and we encourage interested groups to investigate the model's behavior through additional sensitivity experiments.

Lastly, we designed an analysis to diagnose which input variable or combination of input variables to CFFWIS is most responsible for the projected changes we observed. This was done by recalculating late-century FWIs for four cases. By using late-century values for three of the four input variables (i.e., temperature, relative humidity, wind speed, precipitation), we substituted historical values for the final variable and recalculated FWIs. These recalculations were compared with actual late-century projections using simple percentage change calculations for annual maximum FWIs. Figure 9 spatially depicts these four recalculations. For example, the "temperature" subplot in Fig. 9 uses recalculated FWIs computed with historical values of temperature and late-century values of precipitation, wind speed, and relative humidity (determined by the Clausius-Clapeyron relation using late-century values of specific humidity and pressure and historical values of temperature). For the "relative humidity" subplot, also in Fig. 9, we investigated how the role of relative humidity affects late-century fire risk. For this case, we isolated specific humidity's effects on relative humidity and recalculated relative humidity using historical specific humidity and late-century temperature and pressure. Using this method allowed us to preserve the seasonality of the input variables and the respective climate changes in each season rather than broadly applying percent increases or decreases to every grid cell for the whole period.

Meteorological variables which elevate wildland fire risk often have aggregated contributions with respect to fire risk and are difficult to parse (Parisien et al. 2011). Our recalculations of FWIs using historical parameters in Fig. 9 show that temperature is a key variable driving risk in the late-century period. According to Goff et al. (2009), a change in temperature alone is not conducive to increased

Fig. 8 Sensitivity of CFFWIS. Subplots show kernel density estimations of perturbation experiments conducted with varying scalings for each input variable to CFFWIS. Different line types correspond to different perturbations (*solid lines* represent unperturbed runs)
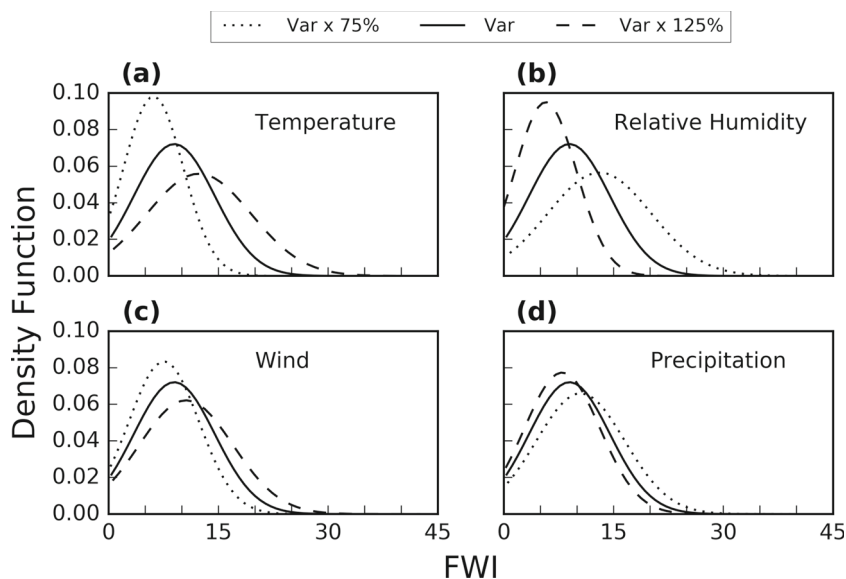
wildland fire risk since this increase will be accompanied by an increase in specific humidity due to the temperature-specific humidity (T-q) feedback implied by the Clausius-Clapeyron relationship (Gaffen and Ross 1999; Dai 2006) thereby limiting the impact of the temperature effect. However, the relative humidity subplot in Fig. 9 indicates that specific humidity does contribute to increases in late-century wildland fire risk, thus suggesting that the positive

effect that increasing temperatures have on wildland fire risk more than compensates the negative effect that specific humidity plays in decreasing risk.

Little research exists on the changes to near-surface winds in the focus region. Klink (2002) observed twentieth century trends in the distribution of wind speeds in Minnesota and referred to wind as an "inherently-noisy variable" influenced by local-scale features. Wind's influence
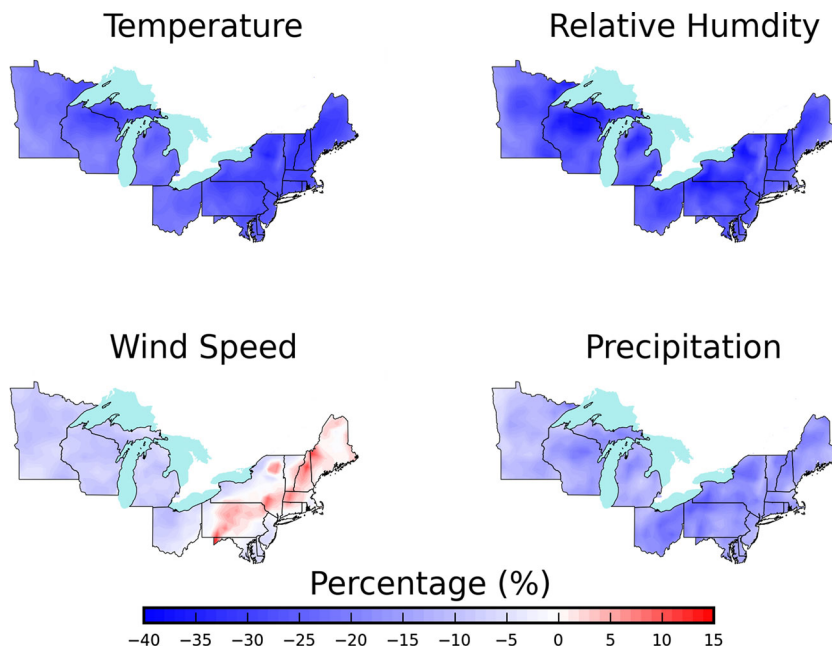

Fig. 9 Input variables to CFFWIS driving change in wildland fire risk. For each subplot, we substituted historical values (1980−2004) of the title variable into the late-century period (2076−2100) to diagnose which input variable was driving the largest changes in wildland fire risk. Percentage differences were found between average annual maximum FWIs from the late-century period with and without

substitution of historical values. An explanation of the color scheme is as follows: percentage decreases *(blue)* indicate that late-century values of the input variable of interest increased wildland fire risk in the late-century period, whereas increases *(red)* indicate that late-century values of the input variable of interest decreased wildland fire risk in the late-century period

on fire risk in the late-century period in Fig. 9 is highly spatially dependent. There are several orographically influenced areas in the Appalachian Mountains which are associated with decreases in fire risk. Conversely, changes in wind in the Great Lakes states are slated to elevate risk. Precipitation's role in increasing wildland fire risk across the focus region is smaller than temperature's and is relatively homogenous (Fig. 9). Recent precipitation distributions across the USA have shown statistically significant trends favoring an increase of precipitation intensity for extreme precipitation events and a decrease for events with lower precipitation amounts (Karl et al. 1999; d'Orgeville et al. 2014). It is documented that precipitation deficits are associated with large fire occurrence and annual area burned (Drever et al. 2008). We speculate that fire risk would increase if the focus region experienced an overall deficit of summertime precipitation with the distribution favoring infrequent, extreme precipitation events; however, additional research is needed to validate this hypothesis. Overall, based on the analysis presented in Fig. 9, we unsurprisingly attribute changes in wildland fire risk primarily to increases in temperature and, to a lesser extent, to decreases in precipitation. Changing wind patterns also will increase wildland fire risk in certain areas.

Recent research on wildland fires and climate change has arrived at similar conclusions as we have; mainly, in the distribution of fire-prone areas and the increasing length of high-risk episodes. Most recent and pertinent are Tang et al. (2015) and Wang et al. (2015). Tang et al. (2015) found that the distribution of historically fire-prone areas does not drastically change during the future. Rather than CFFWIS, Tang et al. (2015) utilized the Haines Index (HI) (Haines 1988) for calculations of historical and future fire risk. HI is based only upon atmospheric stability and moisture content. Tang et al. (2015) used a metric, days per year exceeding an HI threshold, analogous to our use of the annual number of consecutive days above the 95th percentile, and a similar increase of days exceeding this threshold was found during the future. However, Tang et al. (2015) used six different RCM-GCM combinations available from the North American Regional Climate Change Assessment Program (NARCCAP) (Mearns et al. 2009) from CMIP3 (Meehl et al. 2007). NARCCAP's future period spans only 2041-2070 and does not cover the late-century period used in this research where we found the most pronounced changes. Moreover, the study of Tang et al. (2015) examined the contiguous United States as a whole rather than focusing on regional impacts. Wang et al. (2015) calculated wildland fire risk using CFFWIS with inputs from GCMs with a coarser resolution than CORDEX. For their study, start-up calculations used standard values for the moisture codes applied on a constant, single fixed start date unlike our research which initialized CFFWIS on a grid cell by grid cell basis

depending on rigorous temperature thresholds. Lastly, while the conclusions Wang et al. (2015) drew were similar to ours, their research centered on climate change effects on wildland fire risk across Canada's boreal shield.

To reiterate, our findings do not directly translate to specific numerical values for FWIs for a particular year but show general trends and patterns expected to occur by the end of the century. CFFWIS has several limitations which should not be neglected. The largest is that it is a strictly meteorological model with no sensitivity for other main factors driving fire occurrence such as fuel (type, load, connectivity) and ignitions (timing, frequency, type, probability). Assessment of climate change effects on fire risk in the Northeast and Great Lakes regions of the USA is therefore an important first step towards full analysis of future change in fire risk in this region.

4 Conclusions

The expected increases of wildland fire risk pose social impacts with intangible value including loss of life and psychological trauma (Gould et al. 2013). Furthermore, there are socio-economic impacts to the Northeastern United States and Great Lakes region. Commodities such as the timber industry, infrastructure, and personal property all are potential economic losses associated with wildland fires (Gould et al. 2013). The effects of increased wildland fires on ecosystems could be direct and significant. Within the forest, biomass production, carbon sequestration, and nutrient cycles can all be altered by wildland fires, and carbon sinks in post-fire forests are smaller (Weber and Flannigan 1997; Amiro et al. 2001). More tangible effects on ecosystems include habitat loss and a reduction of plant and animal biodiversity (Weber and Flannigan 1997). Beyond the forest, wildfires are primary contributors to particulate matter episodes (Dawson et al. 2014), and emissions from fires can positively change radiative forcing and therefore contribute to net warming effects (Fiore et al. 2015).

We hope that this work will prompt action among both fire management agencies and the scientific community. To adapt to future wildland fire activity, communities can focus on prevention and mitigation of fire risk by managing fuels and increasing awareness. Since most of the land in the focus region is privately owned (unlike in the western United States where many wildfires occur on federal land (Stephens 2005)), the success of prevention and mitigation measures will strongly depend on the commitment of land owners. Early adoption of the FIREWISE community program (www.firewise.org) is recommended to prepare communities for the expected increase in wildfire risk. When fires do occur, fire departments that have traditionally been equipped to deal with structural fires will

require adequate training and equipment to manage and suppress wildfires in the future. The scientific community and modelers, in particular, could also integrate dynamic vegetation models and ignitions data with FWIs to provide regional rasters of wildland fire risk based on daily or seasonal forecasts in order to provide a complete projection of all factors impacting fire risk in the Northeastern and Great Lakes states with future climate change.

References

Amiro BD, Stocks BJ, Alexander ME, Flannigan MD, Wotton BM (2001) Fire, climate change, carbon and fuel management in the Canadian boreal forest. Int J Wildland Fire 10(4):405–413. http://www.publish.csiro.au/?paper=WF01038

Ault TR, Schwartz MD, Zurita-Milla R, Weltzin JF, Betancourt JL (2015) Trends and natural variability of spring onset in the coterminous United States as evaluated by a new gridded dataset of spring indices. J Clim 28(21):8363–8378. doi:10.1175/JCLI-D-14-00736.1

Brutel-Vuilmet C, Ménégoz M, Krinner G (2013) An analysis of present and future seasonal Northern Hemisphere land snow cover simulated by CMIP5 coupled climate models. Cryosphere 7(1):67–80. http://www.the-cryosphere.net/7/67/2013/

Chelli S, Maponi P, Campetella G, Monteverde P, Foglia M, Paris E, Lolis A, Panagopoulos T (2015) Adaptation of the Canadian fire weather index to Mediterranean forests. Nat Hazards 75(2):1795–1810. doi:10.1007/s11069-014-1397-8

Clarke H, Lucas C, Smith P (2013) Changes in Australian fire weather between 1973 and 2010. Int J Climatol 33(4):931–944. doi:10.1002/joc.3480

Clarke HG, Smith PL, Pitman AJ (2011) Regional signatures of future fire weather over eastern Australia from global climate models. Int J Wildland Fire 20(4):550. http://www.publish.csiro.au/?paper=WF10070

Dai A (2006) Recent climatology, variability, and trends in global surface humidity. J Clim 19(15):3589–3606. doi:10.1175/JCLI3816.1

Dawson JP, Bloomer BJ, Winner DA, Weaver CP (2014) Understanding the meteorological drivers of US particulate matter concentrations in a changing climate. Bull Am Meteorol Soc 95(4):521–532. doi:10.1175/BAMS-D-12-00181.1

Dee DP, Uppala SM, Simmons AJ, Berrisford P, Poli P, Kobayashi S, Andrae U, Balmaseda MA, Balsamo G, Bauer P, Bechtold P, Beljaars ACM, van de Berg L, Bidlot J, Bormann N, Delsol C, Dragani R, Fuentes M, Geer AJ, Haimberger L, Healy SB, Hersbach H, Hólm EV, Isaksen L, Kållberg P, Köhler M, Matricardi M, McNally AP, Monge-Sanz BM, Morcrette JJ, Park BK, Peubey C, de Rosnay P, Tavolato C, Thépaut JN, Vitart F (2011) The ERA-Interim reanalysis: configuration and performance of the data assimilation system. Q J R Meteorolog Soc 137(656):553–597. doi:10.1002/qj.828/abstract

DeGroot WJ et al. (1998) Interpreting the Canadian Forest Fire Weather Index (FWI) System. In: Proceedings of the Fourth Central Region Fire Weather Committee Scientific and Technical Seminar. http://www.dnr.state.mi.us/WWW/FMD/WEATHER/Reference/FWI_Background.pdf

d'Orgeville M, Peltier WR, Erler AR, Gula J (2014) Climate change impacts on Great Lakes Basin precipitation extremes: D'Orgeville et al. J Geophys Res: Atmos 119(18):10,799–10,812. doi:10.1002/2014JD021855

Drever CR, Drever MC, Messier C, Bergeron Y, Flannigan M (2008) Fire and the relative roles of weather, climate and landscape characteristics in the Great Lakes-St. Lawrence forest of Canada. J Veg Sci 19(1):57–66. doi:10.3170/2007-8-18313

Fiore AM, Naik V, Leibensperger EM (2015) Air quality and climate connections. J Air Waste Manage Assoc 65(6):645–685. doi:10.1080/10962247.2015.1040526

Flannigan MD, Logan KA, Amiro BD, Skinner WR, Stocks BJ (2005) Future area burned in Canada. Clim Chang 72(1-2):1–16. doi:10.1007/s10584-005-5935-y

Forsythe WC, Rykiel Jr. EJ, Stahl RS, Wu H, Schoolfield RM (1995) A model comparison for daylength as a function of latitude and day of year. Ecol Model 80(1):87–95

Gaffen DJ, Ross RJ (1999) Climatology and trends of US surface humidity and temperature. J Clim 12(3):811–828. doi:10.1175/1520-0442(1999)012

Gallinat AS, Primack RB, Wagner DL (2015) Autumn, the neglected season in climate change research. Trends Ecol Evol 30(3):169–176. http://linkinghub.elsevier.com/retrieve/pii/S0169534715000063

Gao Y, Fu JS, Drake JB, Liu Y, Lamarque JF (2012) Projected changes of extreme weather events in the eastern United States based on a high resolution climate modeling system. Environ Res Lett 7(4):044025. http://stacks.iop.org/1748-9326/7/i=4/a=044025?key=crossref.81de07f01d95bb7a6db4a1d0b075ee60

Giorgi F, Jones C, Asrar GR, et al. (2009) Addressing climate information needs at the regional level: the CORDEX framework. World Meteorological Organization (WMO) Bulletin 58(3):175. http://wcrp.ipsl.jussieu.fr/cordex/documents/CORDEX_giorgi_WMO.pdf

Goff HL, Flannigan MD, Bergeron Y (2009) Potential changes in monthly fire risk in the eastern Canadian boreal forest under future climate change. Can J For Res 39:2369–2380

Gould JS, Patriquin MN, Wang S, McFarlane BL, Wotton BM (2013) Economic evaluation of research to improve the Canadian forest fire danger rating system. Forestry 86(3):317–329. doi:10.1093/forestry/cps082

Guang Y, Xue-ying D, Qing-xi G, Zhan S, Tao Z, Hong-zhou Y, Wang C (2011) The impact of climate change on forest fire danger rating in China's boreal forest. J For Res 22(2):249–257. doi:10.1007/s11676-011-0158-8

Haines DA (1988) A lower atmosphere severity index for wildlife fires. Fire Weather 13(2):23–27

Hamed KH, Rao AR (1998) A modified Mann-Kendall trend test for autocorrelated data. J Hydrometeorol 204:182–196

Hawbaker TJ, Radeloff VC, Stewart SI, Hammer RB, Keuler NS, Clayton MK (2013) Human and biophysical influences on fire occurrence in the United States. Ecol Appl 23(3):565–582. doi:10.1890/12-1816.1/full

Hayhoe K, Wake CP, Huntington TG, Luo L, Schwartz MD, Sheffield J, Wood E, Anderson B, Bradbury J, DeGaetano A, Troy TJ, Wolfe D (2007) Past and future changes in climate and hydrological indicators in the US Northeast. Clim Dyn 28(4):381–407. doi:10.1007/s00382-006-0187-8

Karl TR, Lawrimore J, DelGreco S (1999) United States historical climatology network daily temperature, precipitation, and snow data for 1871–1997. Carbon Dioxide information and analysis center, Publ 4887. http://aprs.ornl.gov/~webworks/cppr/y2002/rpt/101454.pdf

Kendon EJ, Rowell DP, Jones RG, Buonomo E (2008) Robustness of future changes in local precipitation extremes. J Clim 21(17):4280–4297. doi:10.1175/2008JCLI2082.1

Klink K (2002) Trends and interannual variability of wind speed distributions in Minnesota. J Clim 15(22):3311–3317. doi:10.1175/1520-0442(2002)015

Kunkel KE (2004) Temporal variations in frost-free season in the United States: 1895–2000. Geophys Res Lett 31(3). doi:10.1029/2003GL018624

Kunkel KE, Stevens LE, Stevens SE, Sun L, Janssen E, Wuebbles D, Hilberg SD, Timlin MS, Stoecker L, Westcott NE, Dobson JG (2013a) Regional climate trends and scenarios for the U.S. National climate assessment Part 3. climate of the Midwest U.S. NOAA Technical Report NESDIS 142-3 142, no. 3

Kunkel KE, Stevens LE, Stevens SE, Sun L, Janssen E, Wuebbles D, Rennells J, DeGaetano AT, Dobson JG (2013b) Regional climate trends and scenarios for the U.S. National climate assessment: Part 4. Climate of the Northeast U.S. NOAA Technical Report NESDIS 142, no. 4

Lawrence MG (2005) The relationship between relative humidity and the Dewpoint temperature in moist air: a simple conversion and applications. Bull Am Meteorol Soc 86(2):225–233. doi:10.1175/BAMS-86-2-225

Lawson BD, Armitage OB (2008) Northern forestry centre (Canada): weather guide for the Canadian forest fire danger rating system. Northern forestry centre, Edmonton, http://epe.lac-bac.gc.ca/100/200/301/nrcan-rncan/cfs-scf/nor-x/weather_guide/Weatherguide_web.pdf

Maloney ED, Camargo SJ, Chang E, Colle B, Fu R, Geil KL, Hu Q, Jiang X, Johnson N, Karnauskas KB, et al. (2014) North American climate in CMIP5 experiments: Part III: assessment of twenty-first century projections. J Clim 27(6):2230–2270. doi:10.1175/JCLI-D-13-00273.1

Martynov A, Laprise R, Sushama L, Winger K, Šeparović L, Dugas B (2013) Reanalysis-driven climate simulation over CORDEX North America domain using the Canadian Regional Climate Model, Version 5: model performance evaluation. Clim Dyn 41(11-12):2973–3005. doi:10.1007/s00382-013-1778-9

Mearns LO, Jones R, Leung LY, McGinnis S, Nunes AMB, Qian Y (2009) A regional climate change assessment program for North America. EOS 90(36):311–312. http://www.agu.org/pubs/eos/eo0936.shtml

Meehl GA, Covey C, Delworth T, Latif M, McAvaney B, Mitchell JFB, Stouffer RJ, Taylor KE (2007) The WCRP CMIP3 multi-model dataset: a new era in climate change research. Bull Am Meteorol Soc 88:1383–1394

Moriondo M, Good P, Durao R, Bindi M, Giannakopoulos C, Corte-Real J (2006) Potential impact of climate change on fire risk in the Mediterranean area. Clin Res 31(1):85–95. http://www.researchgate.net/profile/Rita_Durao/publication/236107348_Potential_impact_of_climate_change_on_fire_risk_in_the_Mediterranean_area/links/544e2b0f0cf2bca5ce8ef06d.pdf

Moss RH, Edmonds JA, Hibbard KA, Manning MR, Rose SK, van Vuuren DP, Carter TR, Emori S, Kainuma M, Kram T, Meehl GA, Mitchell JFB, Nakicenovic N, Riahi K, Smith SJ, Stouffer RJ, Thomson AM, Weyant JP, Wilbanks TJ (2010) The next generation of scenarios for climate change research and assessment. Nature 463(7282):747–756. doi:10.1038/nature08823

Ning L, Riddle EE, Bradley RS (2015) Projected changes in climate extremes over the Northeastern United States. J Clim 28(8):3289. http://search.proquest.com/openview/b51ea29a8c28e8744de511b418b8732b/1?pq-origsite=gscholar

Parisien MA, Parks SA, Krawchuk MA, Flannigan MD, Bowman LM, Moritz MA (2011) Scale-dependent controls on the area burned in the boreal forest of Canada, 1980-2005. Ecol Appl 21(3):789–805. doi:10.1890/10-0326.1

Peters GP, Andrew RM, Boden T, Canadell JG, Ciais P, Le Quéré C, Marland G, Raupach MR, Wilson C (2013) The challenge to keep global warming below 2 C. Nat Clim Chang 3(1):4–6. http://www.nature.com/nclimate/journal/v3/n1/full/nclimate1783.html

Schwartz MD, Ahas R, Aasa A (2006) Onset of spring starting earlier across the Northern Hemisphere. Glob Chang Biol 12(2):343–351. doi:10.1111/j.1365-2486.2005.01097.x

Schwartz MD, Ault TR, Betancourt JL (2013) Spring onset variations and trends in the continental United States: past and regional assessment using temperature-based indices: Spring Onset Variations and Trends in the continental United States. Int J Climatol 33(13):2917–2922. doi:10.1002/joc.3625

Seneviratne SI, Nicholls N, Easterling D, Goodess CM, Kanae S, Kossin J, Luo Y, Marengo J, McInnes K, Rahimi M, Reichstein M, Sorteberg A, Vera C, Zhang X (2012) Changes in climate extremes and their impacts on the natural physical environment. A Special Report of Working Groups I and II of the Intergovernmental Panel on Climate Change (IPCC), Cambridge University Press, Cambridge, UK, and New York, NY, USA

Šeparović L, Alexandru A, Laprise R, Martynov A, Sushama L, Winger K, Tete K, Valin M (2013) Present climate and climate change over North America as simulated by the fifth-generation Canadian regional climate model. Clim Dyn 41(11-12):3167–3201. doi:10.1007/s00382-013-1737-5

Stephens SL (2005) Forest fire causes and extent on United States forest service lands. Int J Wildland Fire 14(3):213–222

Swain S, Hayhoe K (2015) CMIP 5 projected changes in spring and summer drought and wet conditions over North America. Clim Dyn 44(9-10):2737–2750. doi:10.1007/s00382-014-2255-9

Tang Y, Zhong S, Luo L, Bian X, Heilman WE, Winkler J (2015) The potential impact of regional climate change on fire weather in the United States. Ann Assoc Am Geogr 105(1):1–21. doi:10.1080/00045608.2014.968892

Taylor KE, Stouffer RJ, Meehl GA (2012) An overview of CMIP5 and the experiment design. Bull Am Meteorol Soc 93(4):485–498

Tebaldi C, Knutti R (2007) The use of the multi-model ensemble in probabilistic climate projections. Philosophical Transactions of the Royal Society of London A: Mathematical, Physical and Engineering Sciences 365(1857):2053–2075. http://rsta.royalsocietypublishing.org/content/365/1857/2053.short

Thibeault JM, Seth A (2014) Changing climate extremes in the Northeast United States: observations and projections from CMIP5. Clim Chang 127(2):273–287. doi:10.1007/s10584-014-1257-2

Tian X, McRae DJ, Jin J, Shu L, Zhao F, Wang M (2011) Wildfires and the Canadian Forest Fire Weather Index system for the Daxing'anling region of China. Int J Wildland Fire 20(8):963. http://www.publish.csiro.au/?paper=WF09120

Turner JA, Lawson BD (1978) Weather in the Canadian forest fire danger rating system. a user guide to national standards and practices. Inf. Rep. BC-X-177, Canadian Forestry Service, Pacific Forest Research Centre, Victoria, British Columbia

United States Census Bureau (2013) 2010 Census of population and housing, summary population and housing characteristics. Tech. Rep. CPH-1-1, United States U.S. Government Printing Office, Washington, DC, http://naihc.net/wp-content/uploads/2016/07/AIAN-Housing-Needs-Full-Report_Second-Draft.pdf

van Vuuren DP, Edmonds J, Kainuma M, Riahi K, Thomson A, Hibbard K, Hurtt GC, Kram T, Krey V, Lamarque JF, Masui T, Meinshausen M, Nakicenovic N, Smith SJ, Rose SK (2011) The representative concentration pathways: an overview. Clim Chang 109(1-2):5–31. doi:10.1007/s10584-011-0148-z

Wagner CEV (1987) Development and structure of the Canadian Forest Fire Weather Index System. No. 35 in Canadian Forestry Service, Forestry Technical Report, Canada Communication Group Publ, Ottawa

Wang X, Thompson DK, Marshall GA, Tymstra C, Carr R, Flannigan MD (2015) Increasing frequency of extreme fire weather in

Canada with climate change. Clim Chang 130(4):573–586. doi:10.1007/s10584-015-1375-5

Weber MG, Flannigan MD (1997) Canadian boreal forest ecosystem structure and function in a changing climate: impact on fire regimes. Environ Rev 5(3-4):145–166. doi:10.1139/a97-008

Wilks DS (2011). In: 3rd (ed) Statistical methods in the atmospheric sciences, International Geophysics Series, vol. 100. Academic Press, Oxford, UK

Wotton BM, Flannigan MD (1993) Length of the fire season in a changing climate. For Chron 69(2):187–192. doi:10.5558/tfc69187-2

Wotton BM (2009) Interpreting and using outputs from the Canadian Forest Fire Danger Rating System in research applications. Environ Ecol Stat 16(2):107–131. doi:10.1007/s10651-007-0084-2

Wuebbles DJ, Hayhoe K (2004) Climate change projections for the United States Midwest. Mitig Adapt Strateg Glob Chang 9(4):335–363. doi:10.1023/B:MITI.0000038843.73424.de